Clim Dyn (2017) 48:513–522
DOI 10.1007/s00382-016-3090-y

# Effects of moisture feedback in a frictional coupled Kelvin–Rossby wave model and implication in the Madden–Julian oscillation dynamics

**Fei Liu[1] · Bin Wang[2]**

Received: 11 December 2015 / Accepted: 16 March 2016 / Published online: 26 March 2016
© Springer-Verlag Berlin Heidelberg 2016

**Abstract** The authors extend the original frictional wave dynamics and implement the moisture feedback (MF) to explore the effects of planetary boundary layer (PBL) process and the MF on the Madden–Julian Oscillation (MJO). This new system develops the original frictional wave dynamics by including the moisture tendency term (or the MF mode), along with a parameterized precipitation based on the Betts–Miller scheme. The linear instability analysis of this model provides solutions to elucidate the behaviors of the "pure" frictional convergence (FC) mode and the "pure" MF mode, respectively, as well as the behaviors of the combined FC–MF mode or the dynamical moisture mode. These results show that without the PBL frictional moisture convergence, the MF mode is nearly stationary and damped. Not only does the PBL frictional feedback make the damping MF mode grow with preferred planetary scale but it also enables the nearly stationary MF mode to move eastward slowly, resulting in an oscillation with a period of 30–90 days. This finding suggests the important role of the frictional feedback in generating eastward propagating unstable modes and selecting the preferred planetary scales. The MF process slows down the eastward-propagating short-wave FC mode by delaying the occurrence of deep convection and by enhancing the Rossby wave component. However, the longest wave (wavenumber one) is insensitive to the MF or the convective adjustment time, indicating that the unstable longest wave is primarily controlled by PBL frictional feedback process. Implications of these theoretical results in MJO simulation in general circulation models are discussed.

**Keywords** Madden–Julian Oscillation · Planetary boundary layer · Moisture feedback · Frictional convergence feedback

✉ Fei Liu
liuf@nuist.edu.cn

[1] Earth System Modeling Center and Climate Dynamics Research Center, Nanjing University of Information Science and Technology, Nanjing, China

[2] Department of Atmospheric Sciences and Atmosphere–Ocean Research Center, University of Hawaii at Manoa, Honolulu, HI 96822, USA

## 1 Introduction

The Madden–Julian Oscillation (MJO) is the most energetic intraseasonal cycle in the tropical atmosphere, which has different spectrum characteristics from other convectively coupled equatorial waves (Wheeler and Kiladis 1999). Although the MJO is critical to reginal weather and climate, its fundamental dynamics are still being debated. Until recently explicit MJO simulation has been difficult in the general circulation models (GCMs) (Jiang et al. 2015).

In the frictional convergence (FC) mechanism (Wang 1988b; Wang and Rui 1990), the planetary boundary layer (PBL) will moisten the lower troposphere in front of major MJO convection, and promote deep convection, resulting in an eastward propagation on the intraseasonal time scale. What's more, the longest wave has maximum instability. The weakness of this frictional wave dynamics is that the precipitation in the model is determined primarily by moisture convergence and the moisture tendency term is neglected. This type of representation of precipitation heating is a simple closure scheme, and may be called Kuo-type cumulus parameterization (Wang and Chen 2016).

To understand the effects of moisture feedback (MF), the moisture conservation equation must retain the tendency term even though it might be small compared with

the other terms. A simple theoretical model that isolates the MF is given recently (Sobel and Maloney 2012, 2013). This theoretical model only predicts the moisture perturbation, and the instability originates from several processes such as horizontal advection of seasonal-mean moisture, eddy flux drying and FC feedback. The unstable mode thus obtained is called "the moisture mode", which has maximum low-frequency instability on the planetary scale and propagates eastward slowly.

While both the frictional wave dynamics and moisture process are deemed important to the MJO, only a few theoretical studies focus on their effects on low-frequency dynamics in a unified framework. Majda and Stechmann (2009) propose a theoretical model to couple the free wave dynamics and the MF together. In this theoretical model, the MJO skeleton model, they assume that large-scale heat forcing comes from modulated synoptic-scale wave activity, and link the tendency of planetary-scale wave envelope or diabatic heating with the low-level moisture anomaly. Utilizing this heating parameterization, the model simulates the slow eastward propagation and yields a peculiar dispersion relation in which the frequency is nearly wavelength independent. This model is a neutral model and simulates both the eastward and westward propagation. Liu and Wang (2012) implement PBL dynamics in the skeleton model and reveal that the PBL frictional dynamics provide an instability source to select eastward-propagating planetary-scale MJO skeleton, suggesting the critical role of FC feedback in the MJO dynamics.

In order to include the MF in the MJO dynamics, we develop the original frictional wave dynamics of Wang and Rui (1990) (hereafter the FC model) by including the MF to build a FC–MF model to demonstrate how the moisture process and PBL process impact the MJO dynamics. The original FC model is based on the convectively coupled equatorial waves dynamics (Matsuno 1966), and the precipitation is parameterized by the moisture convergence coming from the lower-troposphere and the PBL. In order to include the MF, we introduce the moisture equation for the lower troposphere, in which the lower-tropospheric moisture can be affected by the diabatic heating and PBL Ekman pumping. A simple Betts–Miller precipitation parameterization (Betts 1986; Betts and Miller 1986) is also used to complete the framework.

Section 2 introduces the models. Section 3 presents the properties of linear normal modes affected by moisture and PBL processes. A physical explanation is offered in Sect. 4. The sensitivity of the solution to cumulus adjustment time scale is discussed in Sect. 5. Conclusions and discussion of the implications of this theoretical work for MJO simulation in GCMs are given in Sect. 6.

## 2 The FC–MF model

### 2.1 Model framework

The MJO circulation is found to be composed of semi-geostrophic Kelvin wave and Rossby wave. The interactions among equatorial waves, PBL process and diabatic heating effect are important for large-scale MJO dynamics (Wang 1988b, 2005; Zhang 2005). Based on these interactions, we extend the original FC model (Wang and Rui 1990), in which the coupling of Kelvin and Rossby waves will excite upward Ekman pumping that moistens the lower troposphere. To study the role of moisture process, the moisture tendency in the moisture perturbation equation needs to be retained, in which case the large-scale precipitation heating must be parameterized. Here, we adopt a simplified Betts–Miller relaxation-type parameterization (Betts 1986; Betts and Miller 1986; Frierson et al. 2004). Details of this FC–MF model can be found in Wang and Chen (2016).

We write the equation in nondimensional units. The velocity scale, $C = 50\ \mathrm{m\ s^{-1}}$, is represented by the speed of the lowest internal gravity waves, the equatorial Rossby deformation radius, $\sqrt{C/\beta} = 1500\,\mathrm{km}$, is the length scale, and $\sqrt{1/C\beta} = 8.5\,\mathrm{h}$ is the temporal scale, where $\beta = 2.3 \times 10^{-11}\ \mathrm{m^{-1}s^{-1}}$ represents the leading-order curvature effect of the Earth at the equator. The non-dimensional FC–MF model representing the large-scale tropical hydrostatic motion can be written for the first baroclinic mode:

$$u_t - yv = -\phi_x$$

$$yu = -\phi_y$$

$$\phi_t + (u_x + v_y) - w = -P_r - \mu\phi$$

$$q_t + \bar{Q}(u_x + v_y) - \bar{Q}_b w = -P_r$$

$$P_r = \frac{1}{\tau}(q + \alpha\phi), \tag{1}$$

where $u$, $v$ are the horizontal winds; $\phi$ is geopotential anomaly; $w$ is vertical velocity caused by the PBL convergence; and $\mu$ is the non-dimensional Newtonian cooling coefficient. Parameter $\bar{Q}$ is the non-dimensional background moisture in the lower troposphere (900–500 hPa), and $\bar{Q}_b$ is the non-dimensional background moisture in the PBL (1000–900 hPa); both are functions of surface specific humidity $q_s$ correlated well with SST

$$q_s(SST) = (0.94 \times SST(^\circ C) - 7.64) \times 10^{-3}, \tag{2}$$

and the vertical profile of the basic-state specific humidity is derived based on the observation that atmospheric

**Table 1** Parameters and their default values used in the experiments

| Parameter | Description | Typical value used (non-dimensional) |
|---|---|---|
| $\bar{Q}$ | Background moisture in lower troposphere (900–500 hPa) | 0.9 (7.3 g kg$^{-1}$) |
| $\bar{Q}_b$ | Background moisture at the BL (1000–900 hPa) | 1.8 (14.6 g kg$^{-1}$) |
| $\mu$ | Newtonian cooling coefficient | 0.18 ($6 \times 10^{-6}$ s$^{-1}$) |
| $E$ | Ekman number in the BL | 1.1 (1/8 h) |
| $d$ | Boundary layer depth | 0.25 (1 km) |
| $\alpha$ | Moisture reference coefficient | 0.1 |
| $\tau$ | Convective adjustment time | 0.25–1.5 (2–12 h) |

absolute humidity over tropical ocean decays exponentially with a water vapor scale height of 2.2 km (Tomasi 1984). In this work a uniform warm SST of 29.5 °C is used, thus the $\bar{Q}$ and $\bar{Q}_b$ are also spatially uniform. The SST is warmest in the tropics, which becomes cold poleward and the e-folding damping scale is 30° (Kang et al. 2013). $P_r$ is the precipitation associated with the diabatic heating of deep convection. $\alpha$ is the coefficient of reference moisture profile measuring relative contribution of the environmental buoyancy to the Convective Available Potential Energy (CAPE) parameterization. $\tau$ denotes the convective adjustment time, which measures how long the convection releases CAPE and relaxes moisture to its reference state. A small $\tau$ implies an intense cumulus activity and a rapid atmospheric adjustment toward the quasi-equilibrium reference state, while a large $\tau$ means that thermodynamics is less tightly constrained (Neelin and Yu 1994). Here, we assume a slow adjustment, thus $\tau = 12$ h is typically used in agreement with the observation (Bretherton et al. 2004). In a theoretical model of "moisture mode" theory, a value of 1 day is used for the convective adjustment time (Sobel and Maloney 2013). Sensitivity experiments with different adjustment times will be presented.

In the well-mixed PBL, the movement is driven by the pressure anomaly, which is assumed to equal to that of the lower troposphere. $w$ has the form of (Liu and Wang 2012)

$$w = d(d_1\phi_{xx} + d_2\phi_x + d_1\phi_{yy} + d_3\phi_y), \tag{3}$$

where $d_1 = e/(e^2 + y^2)$, $d_2 = -(e^2 - y^2)/(e^2 + y^2)^2$ and $d_3 = -2ey/(e^2 + y^2)^2$. $d$ is the non-dimensional PBL depth. $e$ is the Ekman number in the PBL. Taking the longwave approximation or semi-geostrophic approximation in the PBL, Eq. (3) becomes

$$w = d(d_1\phi_{yy} + d_3\phi_y). \tag{4}$$

Numerical computation shows that the PBL longwave approximation is a good approximation to the full PBL (Wang and Rui 1990). Table 1 gives the typical values of these parameters.

The evaporation-wind feedback is an important mechanism for the MJO dynamics, and this mechanism, however, is mean low-level flow dependent (Emanuel 1987; Neelin et al. 1987; Wang 1988a). Contrary results are also obtained by the evaporation mechanism. In an eastward mean low-level flow, the wind-evaporation feedback is found to induce the unstable westward propagation in the "moisture mode" (Sobel and Maloney 2012), while the unstable eastward propagation is obtained when the air-sea interaction is also included (Wang and Xie 1998; Liu and Wang 2013). This complicated wind-evaporation feedback should be discussed in the future works.

### 2.2 Model calculation

This linear system composed of Eqs. (1–4) can be calculated through solving the eigenvalue problem. For this linear system, we assume that the solution has a structure of $e^{i(kx-\sigma t)}$, where $\sigma$ are the frequency, and $k$ the wavenumber, thus the perturbations propagate with a phase speed of $\mathrm{Re}(\sigma)/k$ and a growth rate of $\mathrm{Im}(\sigma)$. This linear system can be transferred onto the frequency-wavenumber field. Thus we obtain a linear matrix of for these five predicted variables. For each wavenumber, the eigenvalue and eigenvector are solved by the matrix inversion method. For simplicity, we use the parabolic cylinder functions to expand the meridional structure and only the first 3 lowest meridional modes are kept. In physics, this means that we only keep the lowest meridional modes of the Rossby and Kelvin waves. The high-frequency waves are filtered out by the longwave approximation in the model.

### 2.3 Three versions of the FC–MF model

To identify the roles of the FC feedback, the MF and the combination of these two feedbacks, we examine three versions of the FC–MF model. The first model version is the FC feedback model in which the moisture tendency term of the moisture equation and the Betts–Miller parameterization are neglected. In this model version, the cumulus parameterization is a simplified Kuo-type Scheme. This FC model is used to isolate the effects of the PBL dynamics. The second version is the MF model, in which the

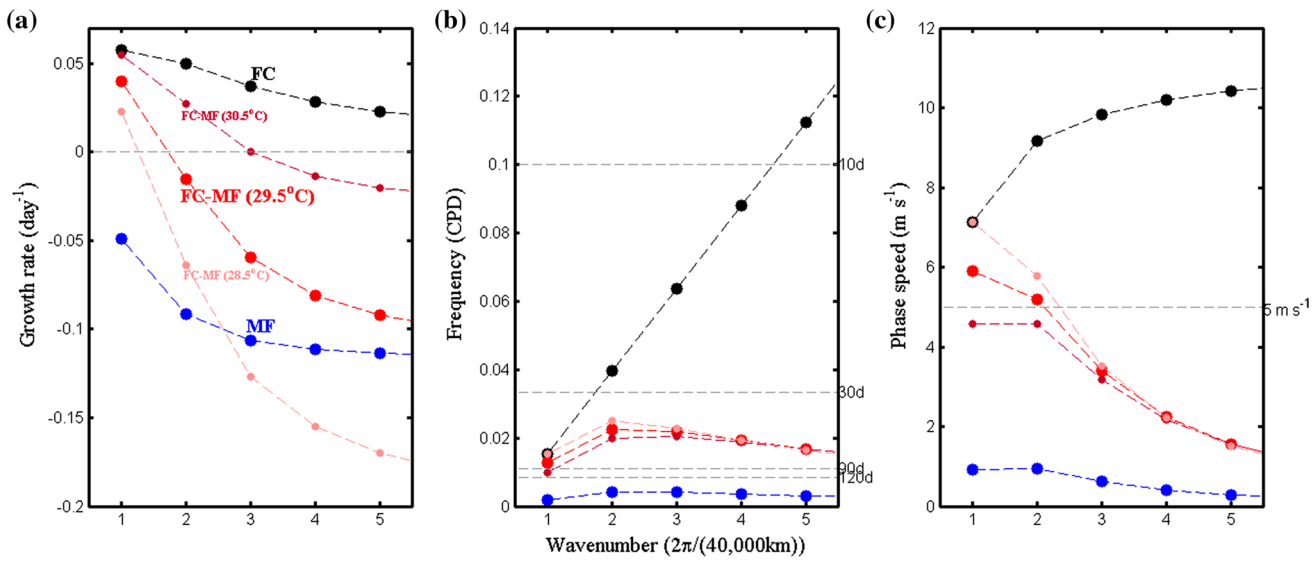


**Fig. 1** **a** Growth rate (day$^{-1}$), **b** frequency (cycle per day) and **c** phase speed (m s$^{-1}$) as functions of wavenumber obtained from three theoretical models, namely, the Frictional Convergence (FC; *dark*), Moisture Feedback (MF; *blue*) and combined FC–MF (*red*) models with a standard SST of 29.5 °C. The results from the combined FC–MF model with a warm SST of 30.5 °C and a cold SST of 28.5 °C are also shown. The definitions of the three models are given in Sect. 2.3

moisture tendency is retained using the Betts–Miller type parameterization, but the PBL dynamics is neglected by setting $w = 0$. This MF model isolates the effects of the MF. Since the "moisture mode" theory has no free tropospheric dynamic feedback, the MF model used here extends the empirical model of the "moisture mode" by including free tropospheric wave dynamics. The last version is a full model presented in Sect. 2.1, in which both the PBL dynamics and the simplified Betts–Miller scheme are included. Namely, the full model contains both the FC feedback and the MF feedback.

## 3 Linear analysis: instability and propagation

Figure 1 compares the linear wave oscillation growth rates and frequency in the FC, the MF and the FC–MF models. Without the moisture process, the FC model yields growing modes with the longest wave (wavenumber one) being the most unstable mode (Fig. 1a). So, the FC feedback selects the longest wave in terms of instability. The longest wave also possesses a reasonable periodicity between 30–90 days (Fig. 1b). However, the period of the FC mode decreases with decreasing wavelength. On the other hand, without the PBL dynamics, the MF model produces only damping modes (Fig. 1a), and the frequency is very low; as a result, the period of the MF modes is longer than 120 days for all wavenumbers (Fig. 1b), suggesting that the MF in the present formulation cannot generate instability and the resulted modes are nearly stationary. In the absence of the wave dynamics feedback, the "moisture mode" theory also presents such a low-frequency mode (Sobel and Maloney 2012, 2013). When both the PBL and moisture processes are included, as in the FC–MF model, the most unstable wavenumber is one, so the longest wave is the fastest growing mode and the only unstable mode as the other shorter waves are damping modes. This behavior is similar to the FC mode with a systematically reduced growth rate. Comparing the three curves in Fig. 1a, we see that the instability in the FC–MF model is rooted in the FC feedback, while the MF tends to reduce the growth rate. As for the period, the low-frequency modes produced by combined FC–MF effect are all within 30–90 days.

From Fig. 1a, we note that these three model versions reproduce different unstable modes. In the FC model, all eastward-propagating modes are unstable and long waves have stronger instabilities than short waves. In the MF model, however, only damping modes exist, in which short waves are damped more quickly. In the FC–MF model, only wavenumber one is unstable when both moisture and PBL process are included. This suggests that it is the FC feedback that is the origin of the instability.

The free troposphere is usually stable when $\bar{Q} < 1$, without including other mechanisms such as the longwave radiation feedback, evaporation feedback, etc. The PBL convergence induced in the coupling of Kelvin and Rossby waves will moisten the lower troposphere to support the development of precipitation anomalies. Thus, the FC model yields unstable eastward-propagating modes for all wavenumbers and the longwave approximation in the

PBL is not favorable for shortwaves and selects long waves for strong instability. This result is in broad agreement with previous work by Wang and Rui (1990).

When the moisture feedback process is included, the precipitation represented by Betts–Miller relaxation-type parameterization acts as a strong damping factor, i.e., precipitation consumes moisture, which means any disturbance would be damped without the presence of other unstable mechanisms. Thus, the MF model has only damping modes. Of many processes destabilizing the moisture mode, we focus on the PBL process here. In the FC–MF model, inclusion of PBL moisture convergence provides an instability source and destabilizes wavenumber one. Why does the combination of positive PBL feedback and negative MF select the planetary wave for strong instability? This will be discussed in the next section.

From Fig. 1b, we note the FC–MF mode presents a dispersion relation like that simulated by the MF model, while the inclusion of PBL process accelerates the eastward propagation speed, resulting in an oscillation on the intraseasonal time sale, i.e., 30–90 days. The wavelength-independent dispersion relation in the intraseasonal temporal domain is also simulated by the MJO skeleton model, in which precipitation is parameterized to lag the moisture anomalies (Majda and Stechmann 2009). In summary, comparison of the solutions between the MF and FC–MF models indicates that the PBL process is critical to generating the eastward propagation, while the difference between the FC model and the FC–MF model shows that the moisture process mainly acts to slow down short waves and leaves wavenumber one much less affected (Fig. 1c).

In this theoretical model, the growth rates are parameters dependent. A stronger growth rate is generated by a warmer SST (Fig. 1a), and the effect of SST on the growth rates is especially significant for shortwaves. For the eastward propagation, the planetary-scale waves are slowed down over the warmer SST and shortwaves are less affected (Fig. 1b, c).

## 4 Physical explanation

Positive eddy available potential energy (EAPE) is necessary for destabilizing the atmosphere, which requires positive covariance between perturbation temperature and diabatic heating associated with large-scale precipitation anomalies. The EAPE is defined by $-\overline{P_r\phi}$ averaged over one wavelength (Wang and Rui 1990). Keep in mind for the first baroclinic mode $\phi = -\theta$, where $\theta$ is the non-dimensional temperature anomaly.

Before analyzing EAPE, we first check how the horizontal structure, especially the phase relationship between different vertical layers, is affected by the PBL dynamics and the MF.

### 4.1 Horizontal and vertical structures

Figure 2 shows the horizontal structures including phase relationship between the PBL and free troposphere of the unstable eastward-propagating wavenumber one in the FC model and the FC–MF model. The damped solution of the MF mode is also shown for comparison. In the FC model, coupling of equatorial Kelvin and Rossby waves can be found (Fig. 2a). The equatorial Kelvin waves propagate eastward, while the Rossby waves propagate westward, which results in a Gill-like pattern (Gill 1980). It is worth mentioning that the PBL upward pumping leads the major convection, which is in a broad agreement with the MJO observation (Hendon and Salby 1994; Sperber 2003). In the MF model without the forcing of PBL moisture convergence (Fig. 2b), the equatorial low-pressure anomalies have a phase lag of $\pi$ with the major convection, and the off-equatorial Rossby-gyre pair is enhanced. Finally, the FC–MF model simulates similar structures as those shown in the FC model, and it has a Gill-like horizontal structure and a vertical tilt characterized by the leading PBL upward moisture transfer to the east of the major convection (Fig. 2c).

These results imply that for both unstable modes in the FC and the FC–MF models, a phase lag between the PBL and free troposphere exists. This vertically-tilted structure contributes to destabilizing the atmosphere and generating the instability.

### 4.2 Energetic analysis

Since the PBL dynamics introduces the vertical tilt, while the MF does not, they should act differently in producing the EAPE. Figure 3 shows the zonal distribution of EAPE in the FC, the MF and the FC–MF model versions. In the FC model, strong positive EAPE is generated in front of the convective center, with a phase lag of about $\pi/4$, while to the west, very weak negative EAPE occurs (Fig. 3a). In the MF model, strong negative EAPE is generated in the convective center and is out of phase with precipitation (Fig. 3b). The FC–MF model gives similar results as the FC model, and positive EAPE is generated in front of the major convection, with a phase lag of less than $\pi/4$ (Fig. 3c). The PBL dynamics is again found to be the instability source for the eastward propagation. The moisture transferred by the PBL will warm the middle troposphere as a direct forcing, while it tends to moisten the lower troposphere before enhancing precipitation in the FC–MF model. This PBL moisture convergence adds additional energy to the free troposphere that is usually stable for the wave-CISK theory

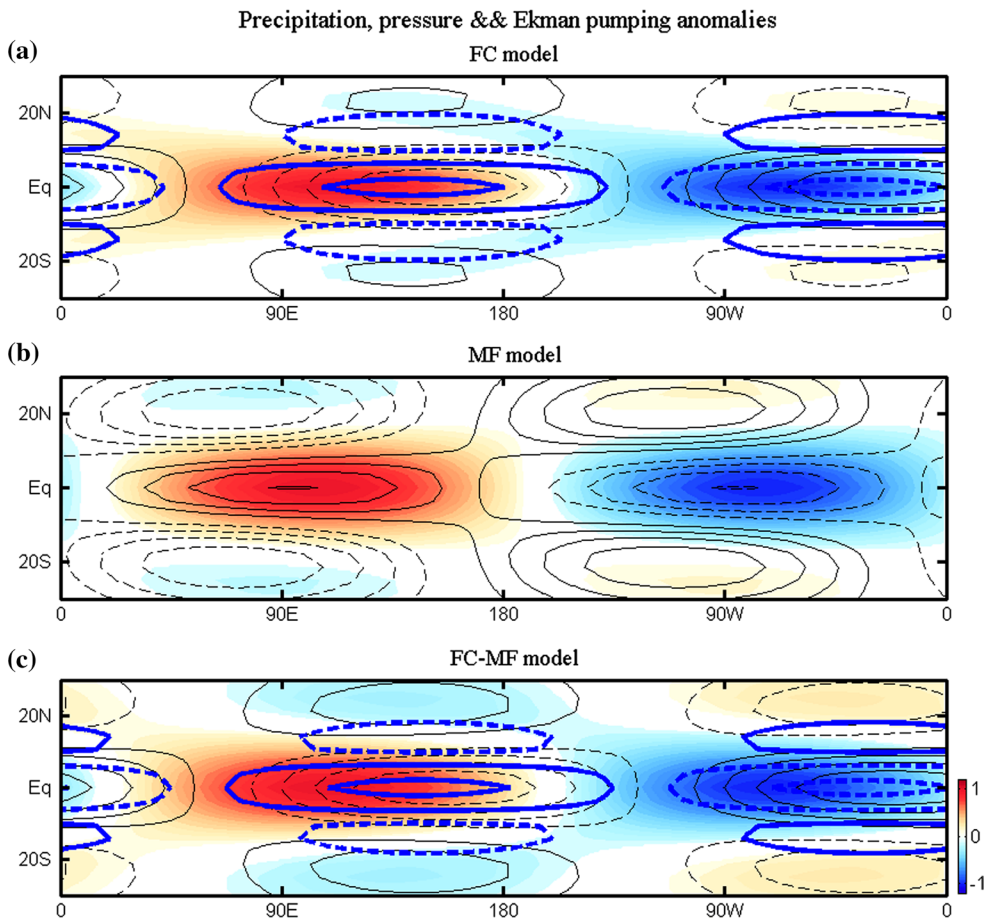


**Fig. 2** Horizontal structures of normalized precipitation anomalies (*shading*), lower tropospheric geopotential height anomalies (*black contours*) and Ekman pumping velocity (*blue contour*) for eastward-propagating, unstable wavenumber-one mode obtained from **a** the FC model, **b** the MF model and **c** the FC–MF model. The contour interval is one-fifth of the maximum amplitude of the anomaly, and zero contour is not shown. The *thick blue contours* denote upward (*solid*) and download (*dashed*) Ekman pumping with 0.2 and 0.8 of the amplitude

(Wang and Rui 1990). Since the Betts–Miller parameterization is a strong negative feedback and the moisture is reduced quickly by the precipitation, only negative EAPE can be generated.

Different wavelength selection in terms of instability from Fig. 1a leads to examination of the generation of EAPE under different scales. Figure 4 shows zonally-averaged EAPE for different wavenumbers in the FC, the MF and the FC–MF model versions. In the FC model, strongest positive EAPE is generated for wavenumber one at the equator, and short waves have small EAPE (Fig. 4a). The positive EAPE generated by the PBL dynamics is the largest at the equator and decays poleward quickly. In the MF model, strong negative EAPE is generated for all wavenumbers near the equator, and the EAPE differences for different wavenumbers only occur in the subtropics (Fig. 4b). In the FC–MF model, only wavenumber one has strong positive EAPE at the equator, while short waves have strong negative EAPE (Fig. 4c). These results imply that the strong positive PBL feedback for long waves can overwhelm the negative MF and generate positive EAPE at the equator, while the positive PBL feedback is weak for short waves, and strong negative MF dominates, which generates negative EAPE in the FC–MF model.

In this work, the vertical tilt indicates the vertical difference between the PBL and the lower troposphere. The backward-tilted vertical profile of moisture, or the positive covariance between the second baroclinic modes of heating and temperature anomalies, is found to generate positive EAPE and amplify the MJO disturbance (Fu and Wang 2009; Zhang and Song 2009; Seo and Wang 2010; Holloway et al. 2013). This vertical-tilted structure, induced by the second baroclinic mode (Mapes 2000; Majda and Biello 2004; Khouider and Majda 2006; Kuang 2008; Wang and Liu 2011), will be added into the current theoretical framework in our future work.

### 4.3 Phase speed

The phase speeds of eastward propagating short waves are much reduced by the inclusion of the MF (Fig. 1c), while the phase speed of wavenumber one is less affected. To explain the role of the MF in changing phase speed, the phase lag between the PBL and troposphere as well as the Rossby–Kelvin wave coupling is re-examined because they all affect the eastward propagation speed. Figure 5 shows how the MF changes the phase lag between the upward Ekman pumping and precipitation center and how the ratio

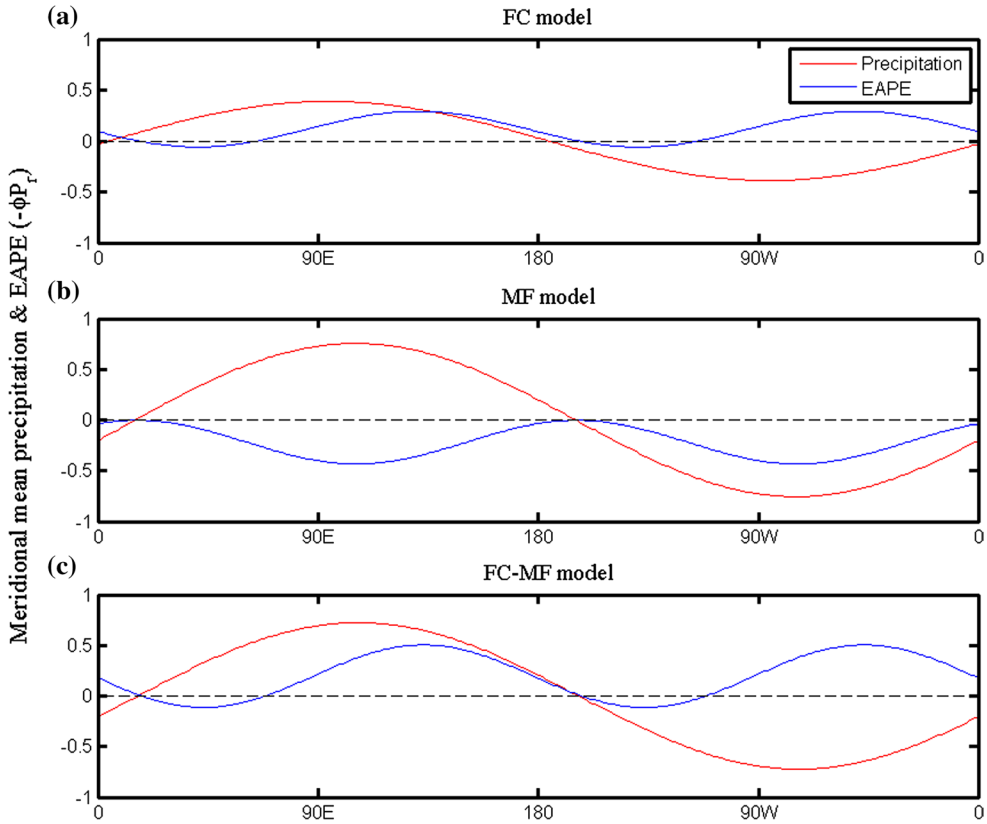


**Fig. 3** Phase relationships between meridionally-averaged (30°S–30°N) precipitation anomalies (*red*) and eddy available potential energy (EAPE $-\phi P_r$; *blue*) for eastward propagating wavenumber-one mode in **a** the FC model, **b** the MF model and **c** the FC–MF model

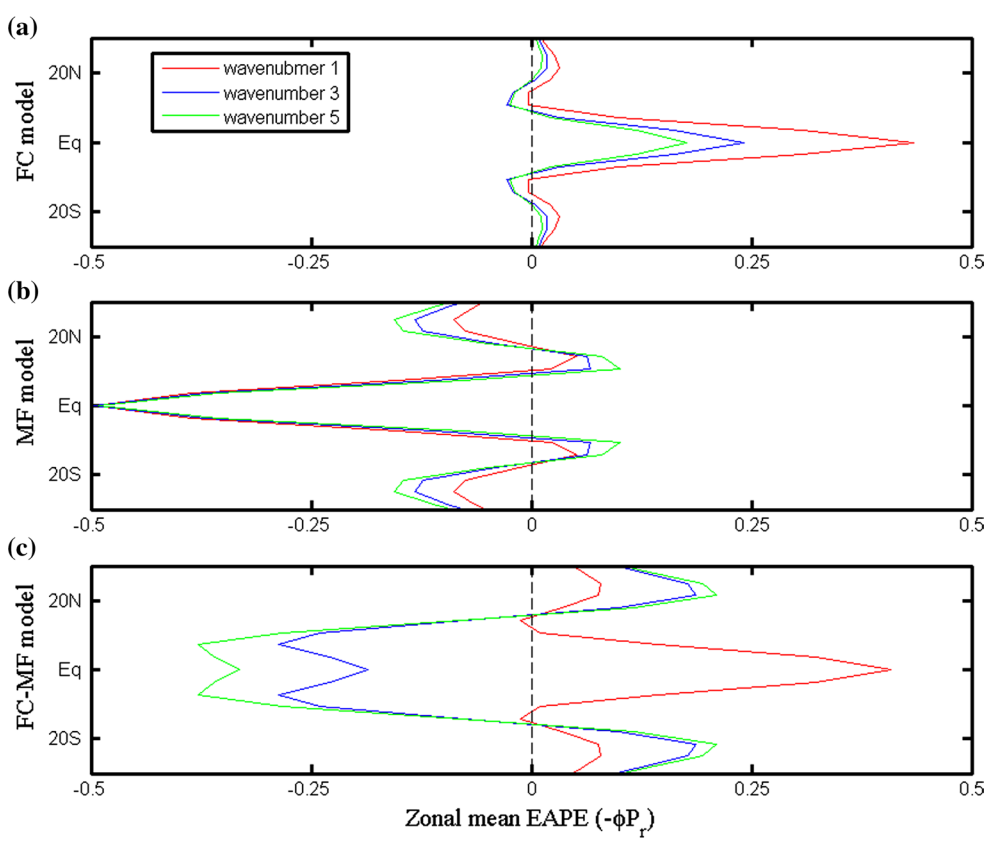


**Fig. 4** Zonally-averaged EAPE of eastward propagating wavenumber-one, -three and -five modes in **a** the FC model, **b** the MF model and **c** the FC–MF model

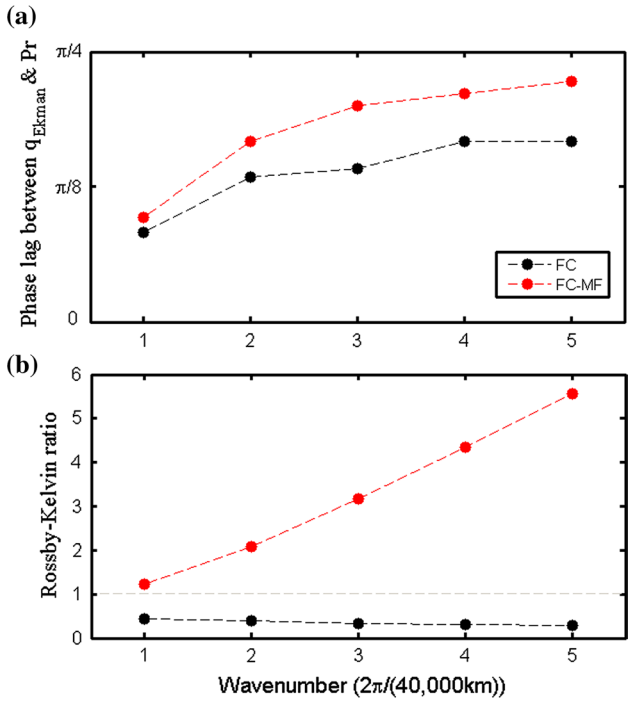


**Fig. 5** **a** Phase lags between equatorial Ekman pumping and convective center and **b** Rossby–Kelvin ratios as a function of wavenumber in the FC (*dark*) and FC–MF (*red*) models, respectively. The Rossby–Kelvin ratio is defined by the ratio of the maximum pressure anomalies between the off-equatorial (15°–25°N) and equatorial (5°S–5°N) regions

of Rossby component to Kelvin component is affected by the MF. Compared to the FC model, the phase lag between the upward Ekman pumping and the major convection is much increased for short waves (Fig. 5a), and the Rossby component in the Rossby–Kelvin wave coupling is also enhanced for short waves in the FC–MF model when the MF is included (Fig. 5b). The phase lag and the Rossby–Kelvin ratio are less affected for wavenumber one. For short waves, the increased phase lag between the upward Ekman pumping and major convection means that the deep convection is delayed by moisture process, which contributes to the slowdown of eastward propagation (Liu et al. 2015). Since the equatorial Rossby waves propagate westward, the enhanced Rossby component in this coupled system also contributes to the slowdown of eastward propagation.

## 5 Sensitivity experiments

In the Betts–Miller parameterization, the convective adjustment time $\tau$ is a critical parameter, which measures the time scale over which convection releases CAPE and moisture is relaxed to its reference state. It is therefore important to understand different solutions of FC–MF model evolvement under different convective adjustment times.

Sensitivity experiments on the convective adjustment time are carried out using the FC–MF model. Figure 6

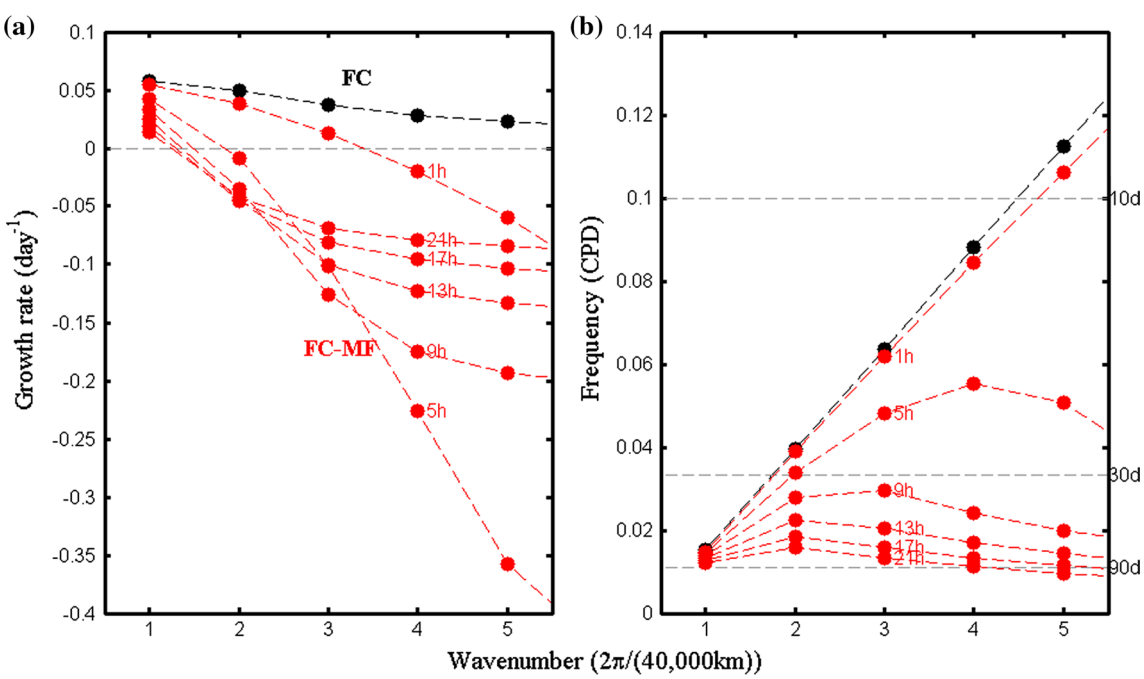


**Fig. 6** Sensitivity of the FC–MF (*red*) model to different convective adjustment times. Linear wave oscillation **a** frequency and **b** growth rate as a function of wavenumber for the MF–KR model with different convective adjust times of 1, 5, 9, 13, 17 and 21 h. The solution of the FC (*dark*) model is drawn as a reference

exhibits how the simulated growth rate and frequency changed by different convective adjustment time. The simulated growth rate and frequency depend heavily on the convective adjustment time for short waves, while wavenumber one is less changed. For a quick adjustment process, the FC–MF model simulates similar growth rate and frequency distribution as those of the FC model. The long waves have a stronger growth rate than the short waves (Fig. 6a), and the frequency increases with wavenumber (Fig. 6b). When the adjustment process is slow, short waves are much suppressed and their frequencies are also largely reduced. This result implies that the moisture process with a long convective adjustment time tends to slow down the short waves, resulting in an intraseasonal oscillation time scale; meanwhile it also strongly damps short waves. The MF process with quick convective adjustment time moderately changes the Rossby–Kelvin coupled system in the FC model. By using a long convective adjustment time of 1 day, a low-frequency motion is simulated by the "moisture mode" theory (Sobel and Maloney 2013). Although Betts and Miller (1986) suggest that an appropriate value of $\tau$ is about two h, the convective adjustment time for the intraseasonal time scale needs more observations.

## 6 Concluding remarks

We have constructed a simple theoretical framework that may be useful for exploring moisture process and PBL process associated with MJO development and propagation. This framework is based on the equatorial Kelvin–Rossby waves coupling and incorporates PBL moisture convergence and moist process. Inclusion of moist process is done by keeping the moisture tendency term in the moisture equation, and this tendency is affected by PBL moisture convergence and by precipitation based on the Betts–Miller parameterization.

In the FC model, instant excitement of convective heating by PBL moisture convergence, i.e., the Kuo-type parameterization (Wang and Chen 2016), yields high-frequency short waves and shows a linear dispersion relationship, in which frequency increases with wavenumber. The PBL process also selects planetary wave to have the maximum instability in the FC model, in agreement with previous work (Wang and Rui 1990). In the MF model without the PBL dynamics, the nearly-stationary modes with oscillations longer than 120 days are strongly damped by the parameterized convective heating in the Betts–Miller scheme.

Introduction of PBL process in the FC–MF model is shown to accelerate these nearly-stationary modes from the MF model and results in an oscillation on the intraseasonal time scale, which also destabilizes wavenumber one by providing additional moisture to support the growth of convection. Compared to the FC model, although the MF reduces the phase speed and instability of short waves heavily, the planetary waves, especially wavenumber-one wave, are less affected by the MF in the FC–MF model; thus, a realistic dispersion of the MJO is simulated by the FC–MF model.

In the original framework focusing on the wave dynamics (Wang and Rui 1990; Wang and Li 1994), the Kelvin and Rossby waves are coupled with precipitation heating by the PBL moisture convergence, and the unstable eastward propagation with a Gill-Like horizontal structure can be simulated. This wave dynamics, however, can only simulate low-frequency wavenumber one in the intraseasonal range, and the frequency of shortwaves from wavenumber two is much higher than that of the MJO. This caveat is remitted when the MF is included.

In both the MF model and the "moisture mode" of Sobel and Maloney (Sobel and Maloney 2012, 2013), the low-frequency mode with a period longer than 120 days has been simulated. This low-frequency mode, however, is unstable in the "moisture mode" and is damped in the MF model, because some positive effective sources of moist static energy, such as zonal advection of mean moisture, cloud-radiative feedbacks, modulation of synoptic eddy drying by the MJO-scale wind perturbation, and FC, are parameterized in the "moisture mode", while they are neglected in the MF model. When FC is included in the MF–FC model, the unstable mode is also obtained. What's more, the inclusion of FC also accelerates the eastward propagation into the intraseasonal range in the MF–FC model.

In the framework including both the wave dynamics and moisture process (Majda and Stechmann 2009, 2011; Liu and Wang 2012), the low-frequency eastward propagation in the intraseasonal range is also simulated. In their works the tendency of planetary-scale envelope, acting as the large-scale diabatic heating, is parameterized by the moisture anomaly. Our results based on the Betts–Miller precipitation parameterization show that only slow convective adjustment process in the Betts–Miller scheme can simulate the low-frequency oscillation in the intraseasonal range, and quick adjustment process will weaken the MF and simulate high-frequency shortwaves.

In both observation and simulation of the MJO, the shallow convection, i.e., the congestus and shallow clouds, is observed to prevail in front of the major convection (Benedict and Randall 2007; Zhang and Song 2009; Del Genio et al. 2012). The shallow convection interacting with the PBL will postpone the onset of deep convection. The role of shallow and congestus clouds acts like that of moisture process with slow convective adjustment in the FC–MF model, and PBL will precondition the lower troposphere rather than heating the troposphere directly. Thus, this work

confirms the important role of moisture accumulation and deep convection delay process in explicit MJO simulation in GCMs.

**Acknowledgments** This work was supported by the China National 973 Project (2015CB453200), the National Natural Science Foundation of China (41420104002), Jiangsu Specially-Appointed Professor (R2015T13) and the Natural Science Foundation of Jiangsu province (BK20150907, BK20150062). BW acknowledges support from the National Science Foundation of the US (climate dynamics division Award No. AGS-1540783) and the Global Research Laboratory (GRL) Program of the National Research Foundation of Korea (Grant No. 2011-0021927). This paper is ESMC Contribution No. 096.

## References

Benedict JJ, Randall DA (2007) Observed characteristics of the MJO relative to maximum rainfall. J Atmos Sci 64:2332–2354

Betts A (1986) A new convective adjustment scheme. Part I: observational and theoretical basis. Q J R Meteorol Soc 112:677–691

Betts A, Miller M (1986) A new convective adjustment scheme. Part II: single column tests using GATE wave, BOMEX, ATEX and arctic air-mass data sets. Q J R Meteorol Soc 112:693–709

Bretherton CS, Peters ME, Back LE (2004) Relationships between water vapor path and precipitation over the tropical Oceans. J Clim 17:1517–1528

Del Genio AD, Chen Y, Kim D, Yao M-S (2012) The MJO transition from shallow to deep convection in CloudSat/CALIPSO data and GISS GCM simulations. J Clim 25:3755–3770

Emanuel KA (1987) An air–sea interaction model of intraseasonal oscillations in the tropics. J Atmos Sci 44:2324–2340

Frierson DM, Majda AJ, Pauluis OM (2004) Large scale dynamics of precipitation fronts in the tropical atmosphere: a novel relaxation limit. Commun Math Sci 2:591–626

Fu X, Wang B (2009) Critical roles of the stratiform rainfall in sustaining the Madden–Julian oscillation: GCM experiments. J Clim 22:3939–3959

Gill AE (1980) Some simple solutions for heat-induced tropical circulation. Q J R Meteorol Soc 106:447–462

Hendon HH, Salby ML (1994) The life cycle of the Madden–Julian oscillation. J Atmos Sci 51:2225–2237

Holloway CE, Woolnough SJ, Lister GM (2013) The effects of explicit versus parameterized convection on the MJO in a large-domain high-resolution tropical case study. Part I: characterization of large-scale organization and propagation*. J Atmos Sci 70:1342–1369

Jiang X, Waliser DE, Xavier PK, Petch J, Klingaman NP, Woolnough SJ, Guan B, Bellon G, Crueger T, DeMott C, Hannay C, Lin H, Hu W, Kim D, Lappen C-L, Lu M-M, Ma H-Y, Miyakawa T, Ridout JA, Schubert SD, Scinocca J, Seo K-H, Shindo E, Song X, Stan C, Tseng W-L, Wang W, Wu T, Wu X, Wyser K, Zhang GJ, Zhu AH (2015) Vertical structure and physical processes of the Madden–Julian oscillation: exploring key model physics in cimate simulations. J Geophys Res Atmos 120:4718–4748

Kang I-S, Liu F, Ahn M-S, Yang Y-M, Wang B (2013) The role of SST structure in convectively coupled Kelvin–Rossby waves and its implications for MJO formation. J Clim 26:5915–5930

Khouider B, Majda AJ (2006) A simple multicloud parameterization for convectively coupled tropical waves. Part I: linear analysis. J Atmos Sci 63:1308–1323

Kuang Z (2008) A moisture-stratiform instability for convectively coupled waves. J Atmos Sci 65:834–854

Liu F, Wang B (2012) A frictional skeleton model for the Madden–Julian oscillation. J Atmos Sci 69:2749–2758

Liu F, Wang B (2013) An air–sea coupled skeleton model for the Madden–Julian oscillation. J Atmos Sci 70:3147–3156

Liu F, Chen Z, Huang G (2015) Role of delayed deep convection in the Madden–Julian oscillation. Theor Appl Climatol. doi:10.1007/s00704-015-1587-7

Majda AJ, Biello JA (2004) A multiscale model for tropical intraseasonal oscillations. Proc Natl Acad Sci USA 101:4736–4741

Majda AJ, Stechmann SN (2009) The skeleton of tropical intraseasonal oscillations. Proc Natl Acad Sci USA 106:8417–8422

Majda AJ, Stechmann SN (2011) Nonlinear dynamics and regional variations in the MJO skeleton. J Atmos Sci 68:3053–3071

Mapes BE (2000) Convective inhibition, subgrid-scale triggering energy, and stratiform instability in a toy tropical wave model. J Atmos Sci 57:1515–1535

Matsuno T (1966) Quasi-geostrophic motions in the equatorial area. J Meteorol Soc Jpn 44:25–43

Neelin JD, Yu J-Y (1994) Modes of tropical variability under convective adjustment and the Madden–Julian oscillation. Part I: analytical theory. J Atmos Sci 51:1876–1894

Neelin JD, Held IM, Cook KH (1987) Evaporation-wind feedback and low-frequency variability in the tropical atmosphere. J Atmos Sci 44:2341–2348

Seo K-H, Wang W (2010) The Madden–Julian oscillation simulated in the NCEP climate forecast system model: the importance of stratiform heating. J Clim 23:4770–4793

Sobel A, Maloney E (2012) An idealized semi-empirical framework for modeling the Madden–Julian oscillation. J Atmos Sci 69:1691–1705

Sobel A, Maloney E (2013) Moisture modes and the eastward propagation of the MJO. J Atmos Sci 70:187–192

Sperber KR (2003) Propagation and the vertical structure of the Madden–Julian oscillation. Mon Weather Rev 131:3018–3037

Tomasi C (1984) Vertical distribution features of atmospheric water vapor in the Mediterranean, Red Sea, and Indian Ocean. J Geophy Res Atmos (1984–2012) 89:2563–2566

Wang B (1988a) Comments on "an air-sea interaction model of intraseasonal oscillation in the tropics". J Atmos Sci 45:3521–3525

Wang B (1988b) Dynamics of tropical low-frequency waves: an analysis of the moist Kelvin wave. J Atmos Sci 45:2051–2065

Wang B (2005) Theories. In: Lau K-M, Waliser DE (eds) Intraseasonal variability of the atmosphere-ocean climate system. Springer, Heidlberg

Wang B, Chen G (2016) A general theoretical framework for understanding essential dynamics of Madden-Julian Oscillation. Clim Dyn (**submitted**)

Wang B, Li T (1994) Convective interaction with boundary-layer dynamics in the development of a tropical intraseasonal system. J Atmos Sci 51:1386–1400

Wang B, Liu F (2011) A model for scale interaction in the Madden–Julian Oscillation. J Atmos Sci 68:2524–2536

Wang B, Rui H (1990) Dynamics of the coupled moist Kelvin–Rossby wave on an equatorial β-plane. J Atmos Sci 47:397–413

Wang B, Xie X (1998) Coupled modes of the warm pool climate system. Part I: the role of air–sea interaction in maintaining Madden–Julian oscillation. J Clim 11:2116–2135

Wheeler M, Kiladis GN (1999) Convectively coupled equatorial waves: analysis of clouds and temperature in the wavenumber-frequency domain. J Atmos Sci 56:374–399

Zhang C (2005) Madden–Julian oscillation. Rev Geophys 43:RG2003. doi:10.1029/2004RG000158

Zhang GJ, Song X (2009) Interaction of deep and shallow convection is key to Madden–Julian oscillation simulation. Geophys Res Lett 36:9708